

# MIQM: Multicamera Image Quality Measures

<sup>1</sup>Mr. Rahul P. Bembade, <sup>2</sup>Prof. Pankaj R. Chandre

<sup>1,2</sup>Sharadchandra Pawar College Of Engineering, Dumbarwadi, Otur, Pune.  
University Of Pune

## Abstract

*With the rising demand of multiview application, quality assessment of multicamera images and videos is becoming crucial to the development of these applications. Image quality is depending upon several factors, which may be camera configuration, stability of camera during taking photo, number of cameras, and the calibration process etc. While numerous subjective and objective quality measurement methods have been projected in the literature for all images and all videos from single cameras, no comparable effort has been dedicated to the quality assessment of multicamera images. With the intention of develop an objective metric specially designed for multi camera system, we recognized and quantify two types of visual distortion in multicamera image: one is photometric distortions and another is geometric distortions. The comparative distortion between individual camera scenes is a major factor in determining the overall perceived quality. The distortions can be translated into components like contrast, luminance, edge based structure and spatial motion. We suggest three different indices that can compute these components. We give examples to show the correlation among these components and the corresponding indices. Multicamera image quality measure (MIQM) is calculated by combining three indices which are luminance and contrast index, spatial motion index and edge based structure index. The result and comparison with the other measures, like peak signal-to noise ratio (PSNR), mean structural similarity (SSIM), and visual information fidelity (VIF) prove that MIQM surpass other measure in capturing the perceptual fidelity of multicamera images. And in last, the results against subjective assessment are verified.*

**Keywords:** Fidelity measures, image quality assessments, multicamera arrays, multiview imaging, perceptual quality

## 1. INTRODUCTION

Multicapture of events has become crucial to gratify the demand for advanced immersive multimedia products due to the speedy enhancement in computing current Technologies and electronics world and plummeting camera cost. Advertisement, distance learning, entertainment, video conferencing, surveillance, photography, sightseeing, and medical training etc. are applications include in such product. Multiview is defined as a set of images or videos captured by set of two or more cameras and multiview applications is interactivity is a key advantage. The application users have the liberty of choosing the viewpoint within the captured scene. Multiview applications are not inadequate to free viewpoint, interactive stereo, 3-DTV and panoramic, virtual view

synthesis, stereoscopic video and object tracking [9], [13]. The processing chain of these applications consists of seven process steps which image are capturing process, camera calibration process, scene presentation process, coding process, transmission process, multiview rendering process, and display process [9]. Each and every step in the processing chain gives the perceived quality of the video or image. Multicamera applications are several and each application has its specific means of acquisition, representation, and display. During the last two decade, the main performance metric in multiview video and image processing is subjective evaluation. The subjective evaluation having some disadvantages like it is not efficient and it is time consuming. Subjective evaluation is not useful in the real time environment. The definition of the quality of the perceived multiview video or image is dependent on the means of presentation. There are several means to present multiview videos and images: free viewpoint, interactive stereo, 3-DTV, panoramic, virtual view synthesis, stereoscopic video and object tracking [13]. More than one camera is used to capture a particular scene in the applications of panoramic video. The final outputs come from the cameras are then combined to copy the performance of a much costlier multi mega pixel wide angle video camera. Two cameras are used in communicating stereoscopic video to capture two different views of an object from slightly different positions. Then, a 3-Dimension impression of the scene is created by projecting the 2-Dimension slightly different scenes on the retina of each eye. By using physiological fusing of the stereoscopic pair, the human brain creates the impression of depth. A scene is captured in the case of free viewpoint video by multiple cameras. Through a combination of video sources and some information about camera calibration and scene geometry, free viewpoint video allows the user to navigate through the image by choosing his/her own viewpoint. Finally, in 3-DTV, a scene is captured as in multiple view videos, and one or more 3-D video objects are created. The cameras are arranged with relatively short baseline to synthesize virtual views directly from camera images. Previously mentioned applications share similar acquisition apparatus and precompositing processing block. The acquisition apparatus involves multiple cameras to capture multiple views of a real world scene. The captured views are then photometrically and

geometrically calibrated before being composite to be displayed. Different views captured by different cameras may differ in terms of color, brightness, noise level, and orientation. The calibration process derives the necessary information to map each of the views dimensions into the real world or the reference view dimensions. The perceived scene for each of the multicamera applications is an output of the compositing algorithm, which is generally a function of the captured scenes, camera calibration, and scene geometry. Hence, it is impossible to define a single quality measure that would capture the perceived quality of all multi camera applications. So we define a multi camera image quality measure (MIQM), which was tested and refined for ultrahigh resolution panoramic image applications. The resulting measure captures the visual effects of artifact which are introduced at the acquisition and precompositing processes to predict the composite image quality. The measure was developed based on acquisition and precompositing artifacts to serve as a basis from which we could extend the results to develop quality measures for stereoscopic, panoramic image, free viewpoint, and 3-DTV applications after taking into consideration stereoscopic impairments and synthetic artifacts. In multi camera systems distortions can be classify into two distortions, first is geometric distortion and another is photometric distortion [2]. Multiple image quality measure (MIQM) is consisting of three index measures: first is the luminance and contrast index, second is the spatial motion index, and third is the edge-based structural index. Luminance and contrast index and the edge-based structural index are used to measure photometric distortions where as the spatial motion index and the edge-based structural index are used to measure geometric distortions.

## **2. LITERATURE SURVEY**

Ghassan AlRegib et. al. [1]. In this paper, they show that distortions can be translated into luminance, contrast, spatial motion, and edge based structure components. They propose three different indices that can quantify these components. Then, they combine these all indices into one multicamera image quality measure (MIQM). Results and comparisons with other measures such as peak signal-to noise ratio (PSNR) mean structural similarity (SSIM), and visual information fidelity (VIF) show that MIQM outperform other measures in capturing the perceptual fidelity of multicamera images. G. AlRegib et. al. [2], the author proposed that geometric and photometric distortions are the classifications of distortions in the multicamera system. R. Cutler et. al. [11], the authors proposed an objective quantity metric for Omni directional video. The metric accessed the general quality of the video using no-reference blockiness and blur measure. To show that current single video camera

quality assessment techniques are not adequate for quality assessment of Omni directional panorama video generated by multiple cameras, Leorin et.al [11] used subjective tests. Z. Wang et.al. [12], in their paper authors proposed theory of structural similarity (SSIM) for each and every camera based on the assumption that the human visual system is highly adapted to extract structural information from the viewing field. P. Campisi et. al. [7], the authors in [7] performed quality assessment of stereo image pairs, by using quality metrics of single view for each view. N. Ozbek et. al.[8], the authors assumed that for 3-dimensional visual experience, peak signal to noise ratio (PSNR) of the second view is less important and new measure was included of weighted combination of two PSNR values and jerkiness measure for temporal artifacts. C. Hewage et. al [3] the authors proposed the performed quality assessment of stereo image pairs using single view quality metrics on each view. Numerous combination methods of the quality scores from each and every view were then evaluated to decide the ones that best associated with the subjective scores. The identical level of distortion was applied to both images of the stereo pair and the distortion types were limited to the blur and compression artifacts. J. Starck et. al. [5], the authors propose a free view point video production objective metric. These metrics can be used as a full reference measure of fidelity of aligning the structural details in the presence of approximate scene geometry of the 3-dimensional shapes. A. Tikanmaki, et. al.[4], the authors proposed using conventional single camera quality measures (PSNR and SSIM) for 3-DTV video as a quality measure for video plus depth content, by measuring the quality of the virtual views that are rendered from the distorted color and depth sequences attributes. P.J.Burt et.al. [14], the authors in proposed that the multimedia image was simulated by compositing the sub-images into a one single image mosaic using a multi resolution spline. They also mentioned that the reference image is created by combining all sub-images without any distortion. Distortion may be geometric or photometric or both. C.Tang et.al. [10], the authors proposed an edge based texture model for visual distortion sensitivity in video bit allocation algorithm. By using this model, visual sensitivity model for multicamera image can be derived which is useful in free viewpoint, interactive stereo, 3-DTV and panoramic, virtual view synthesis, stereoscopic video and object tracking. L. Cui et.al. [6], the authors proposed that due to geometric distortions and photometric distortion, loss in structural information occurs and such structural information consist of degradation in texture quality. Calculating the structural similarity (SSIM) over edge maps instead of the actual images leads to better relationship with subjective quality for the SSIM.

3. EXPERIMENTAL RESULTS

3.1 MIQM Approach

The goal of MIQM is to derive a new quality measurement for multi-camera images. Since the quality of images are affected by multiple factors such like number of cameras, camera configuration, calibration process, quality assessment for such an image should take all these into consideration. To design an objective metric for multi-camera images, the visual distortion is identified into two types, photometric distortion and geometric distortion, which can be translated into luminance, contrast, spatial motion and edge-based structure components. The main idea of the paper is to first quantify each component by proposing different index values and then to combine those indexes into one quality, MIQM, to capture the perceptual quality of multi-view images. And calculation on a macro block level is a basic method. MIQM represents measurement that is full-reference and designed to assess multi-view images, where the reference is regarded as the set of images taken by identical cameras. Different distortions are handled in MIQM according to the following method described below

3.1.1 MIQM Results

The results of MIQM can be get by using following steps.

3.1.1.1 Split each image

Split image into two overlapping halves (Left and Right). The amount of overlap should be a design parameter.



Figure 3.1: Result of Function Dist-Free

3.1.1.2 Distortions

A .Function to fulfill the geometric distortion Instead of achieve the perspective geometric distortion and planar geometric distortion separately; we use a general geometric distortion formula to simplify it. We choose different geometric distortion type by sending different parameters to this function

$$y \begin{pmatrix} u_1 \\ u_2 \end{pmatrix} \approx x \begin{pmatrix} u_1 + (u_1 \Delta s_1 - u_2 \Delta \theta + \Delta t_1 - u_2 \Delta s_2 \Delta \theta) \\ u_2 + (u_2 \Delta s_2 + u_1 \Delta \theta + \Delta t_2 + u_1 \Delta s_1 \Delta \theta) \end{pmatrix}$$

In this formula,  $(1+\Delta s_1, 1+\Delta s_2)$ ,  $\Delta \theta$  and  $(\Delta t_1, \Delta t_2)$  are the scaling, rotation and translation factors, respectively. Below are the results that we use this formula to fulfill different geometric distortion type.



Figure 3.2: Three Different Geometric Distortions  
B. Photometric distortion by blurring the image. Below is the “photo-blur” image.

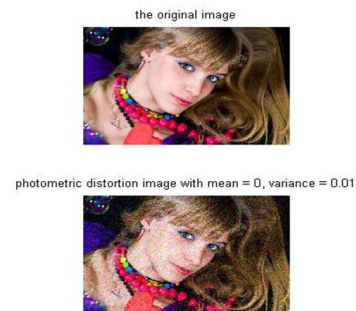


Figure 3.3: Photometric Distortion by Blurring the Images

3.1.1.3 Apply the mosaicking code to create composed image.



Figure 3.4 : Composed Image(a) original left half with rotated right half (angle = 0.05); (b) original left half with scaled right half (scaleX = scaleY = -0.05); (c) original left half image with shifted half image(shiftX = shiftY = 10); (d) original left half with blurred left half image (mean = 0, variance = 0.05) For the following steps, the indexes are generated on the luminance channel.

B.1 Write a code that computes the Luminance and Contrast Index.

B.2 Re-generate the images in Fig.3.5.

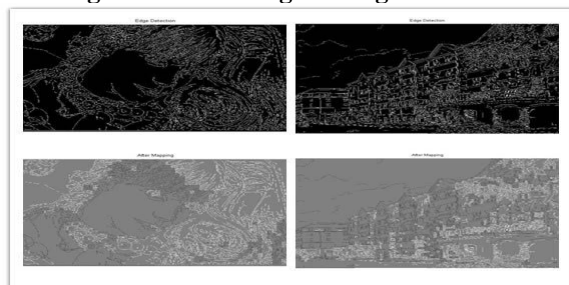
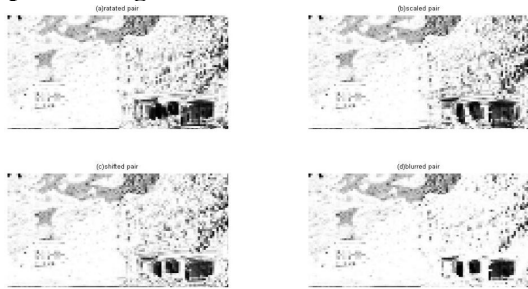


Figure 3.5: Regeneration

The images after mapping are not the same as the corresponding images in the paper, because different levels of distortions are applied in the original image. Before detect the edges, applying a Gaussian smoothing operator will improve the performance. The index values are large in randomly textured regions but small in structural regions.

**B.3 Re-generate the image in Fig.3.6 (b). Base on the four paired image above.**



Since Fig.3.6 uses the Water Front image, here we use the same images for the convenient of comparison. And we use exactly the same four paired parameter as illustrated in part A. In the luminance and contrast index, the darker regions refer to areas of higher distortion. We can obviously find that the right parts corresponding to the blurred views have darker regions than the rights parts distorted by perspective distortion. Therefore, luminance and contrast index can well capture the perceptual distortion of blurred views with focusing on the structural regions, which is vital because sudden local changes in luminance and contrast around structured regions are very annoying.

**B.4 Write your own code to compute the Spatial Motion Index.**

**B.5 Regenerate the image in fig.3.6(c).Base on the four paired image above.**

In spatial motion vector index map, spatial displacements caused by geometric distortions have darker values. The gray regions in above images are a result of mosaicking.

**B.6 Write your own code to compute the Edge Index.**

**B.7 Re-generate the image in Fig.3.6(d). Base on the four paired image above.**

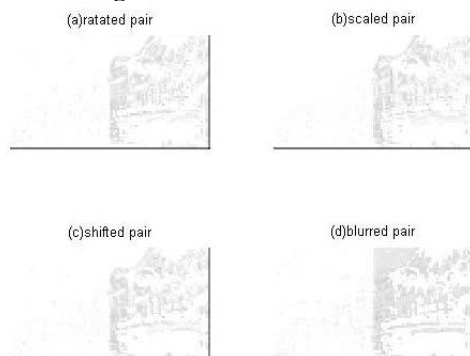


**Fig 3.7: Motion Index Map**

As the images show, it is the blurred view that structural loss represented by the edge-based structural index is concentrating on. Due to structural loss, majority of the image are gray. In the images, the dark pixels are caused

by geometric distortions, which preserve global structures and change the positioning and direction of the structure. Structural losses in geometric distortions may occur frequently around a macroblock boundary in low structured regions.

**B.8 Compute the MIQM and PSNR values as in Fig. 3.7**



**Figure 3.8: Images with Various Distortion Types**

- (a) PSNR= $\infty$  MIQM=1
- (b) PSNR= $\infty$  MIQM=1
- (c) PSNR=19.3367 MIQM=0.7999
- (d) PSNR=15.1667 MIQM=0.7064
- (e) PSNR=17.5265 MIQM=0.6793
- (f) PSNR=15.9538 MIQM=0.7233

**C.1 Compute the SSIM values for the images in Fig. 3.7**

- (a) SSIM=1
- (c) SSIM=0.9168
- (e) SSIM=0.8824
- (b) SSIM=1
- (d) SSIM=0.7906
- (f) SSIM=0.8355

MIQM performs better than SSIM and PSNR on multi-view images. It is a more consistent quality measure.

**C.2 Vary the overlapping region between left and right and re-compute MIQM and PSNR values.**

We can get the value by running nine.m and change related parameters. We change the overlapping to 10%. Then get the corresponding values for PSNR and MIQM as follows. Because the limit of space, the generated images are not showed here. According to the values,

PSNR decreases as the overlapping area become larger for perceptive distortion. And so is the same with MIQM which also become smaller. As for the photometric distortions like Gaussian blur, the PSNR and MIQM do not change largely, which may indicate that PSNR and MIQM is more sensitive to geometric distortion than photometric distortion. And when the distortion becomes severe, both values will decrease.

- (a) PSNR= $\infty$  MIQM=1
- (b) PSNR= $\infty$  MIQM=1
- (c) PSNR=18.9743 MIQM=0.7892
- (d) PSNR=15.0262 MIQM=0.7084
- (e) PSNR=17.5212 MIQM=0.6693
- (f) PSNR=17.1265 MIQM=0.7144

**C.3 Varying the parameters**

We can get the value by running nine.m and change related parameters. In this experiment, we change s=16 to s=32. And we get the following values. When s becomes larger, both PSNR and MIQM increase a little, indicating that increasing s will increase PSNR and MIQM.

- (a) PSNR= $\infty$  MIQM=1
- (b) PSNR= $\infty$  MIQM=1
- (c) PSNR=19.3367 MIQM=0.8349
- (d) PSNR=15.1667 MIQM=0.7497
- (e) PSNR=17.5322 MIQM=0.7540
- (f) PSNR=17.9545 MIQM=0.7700

**3.2OUR Approach**

In our approach of image quality measurement process we perform various quality measurements methods as stated in the proposed approach chapter. Here we are evaluating the results for the various distortions types as propose below

**3.2.1 Perspective Distortions**

For this demonstration we consider two images as shown below



**Fig. 3.9:** Test images for perspective distortion

When we apply the perspective distortions with factor 2 for image (a) then it produces the distorted image and when we measure factor then it yields the measurement index as 1.889. This show our method yields accuracy of 0.9445 for the image (a). When we apply the perspective distortions with factor 5 for image (b) then it produces the distorted image and when we measure factor then it yields the measurement index as 4.566. This show our method yields accuracy of 0.912 for the image (b). The results can be shown in below figure.

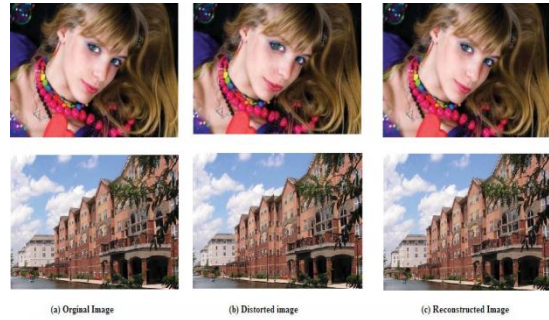


**Figure 3.10:** Image (a) and (b) with perspective distortions results

When we compare our method with the other existed system we got the following table and that can be shown in graph of figure 3.12.

**Table 3.1:** Measurement index comparison of perspective distortion

Image	Original	PSNR	SSIM	MIQM	Our Approach
A	1	19.4249	0.7511	0.6287	0.9445
B	1	15.649	0.4446	0.8223	0.912

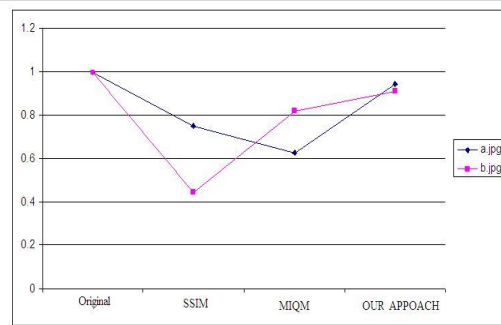


**Figure 3.11:** Perspective Comparison

On observing the graph we can come to a conclusion that our approach values are very nearer to the value 1. So it over perform MIQM for the given images.

**3.2.2 Planar Distortions**

For this demonstration we consider two images as shown below



**Fig. 3.12:** Test images for planer distortion

When we apply the planar distortions with factor 8( as Angle) for image (a) then it produces the distorted image and when we measure factor then it yields the measurement index as 7.639021 This show our method

yields accuracy of 0.9548 for the image (a). When we apply the planar distortions with factor 6 for image (b) then it produces the distorted image and when we measure factor then it yields the measurement index as 4.352576 This show our method yields accuracy of 0.725429 for the image (b). The results can be shown in below figure.

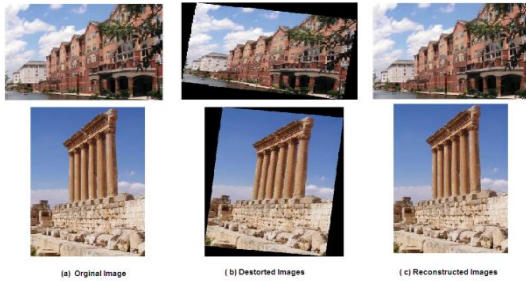


**Figure 3.13:** Image (a) and (b) with planar distortions results

When we compare our method with the other existed system we got the following table and that can be shown in graph of figure 3.14

**Table 3.2:** Measurement index of planar distortion performance

Image name	Distortion applied value	Measured value
Girl	5	5.457361
Building	8	7.639021
Pillar	6	4.352576

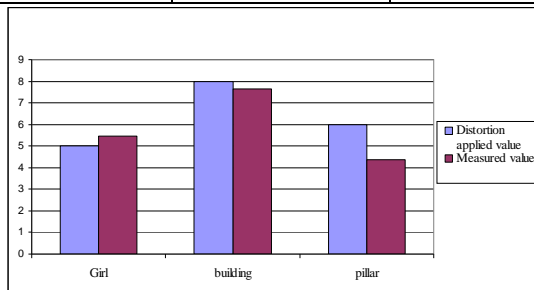


**Figure 3.14:** Planar Performance

On observing the graph we can come to a conclusion that our approach values are very nearer to the original image. So we can conclude that our system performance is well in planar type.

**3.2.3 Photometric Compression Distortions**

For this demonstration we consider two images as shown below



**Fig. 3.15:** Test images for photometric distortion

When we apply the JPEG compression distortions with factor 0.5 for image (a) then it produces the distorted image and when we measure factor then it yields the measurement index as 0.5. This show our method yields accuracy of 1 for the image (a). When we apply the perspective distortions with factor 0.7 for image (b) then it produces the distorted image and when we measure factor then it yields the measurement index as 0.69 This show our method yields accuracy of 0.9857 for the image (b). The results can be shown in below figure.



**Figure 3.16:** Image (a) and (b) with photometric JPEG Compression distortions results

When we compare our method with the other existed system we got the following table and that can be shown in graph of figure 3.18

**Table 3.3:** Measurement index of JPEG Compression distortion performance

Image	Value applied	Value measured
Girl	0.5	0.5
Building	0.7	0.69
Pillar	0.4	0.39

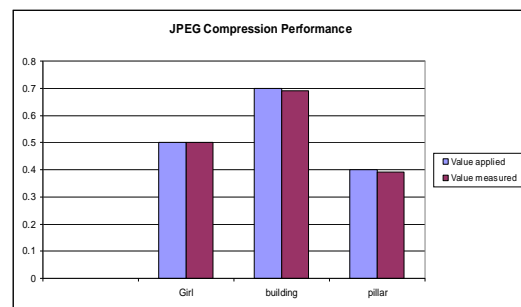


**Figure 3.17:** JPEG Compression distortion Performance

On observing the graph we can come to a conclusion that our approach values are very nearer to the original image. So we can conclude that our system performance is well in JPEG Compression type of distortions.

**Table 3.4:** JPEG Compression comparison with other methods

Image	JPEG Compression				Our Approach
	Original	PSNR	SSIM	MIQM	
Girl	1	28.0633	0.8996	0.6214	0.9875

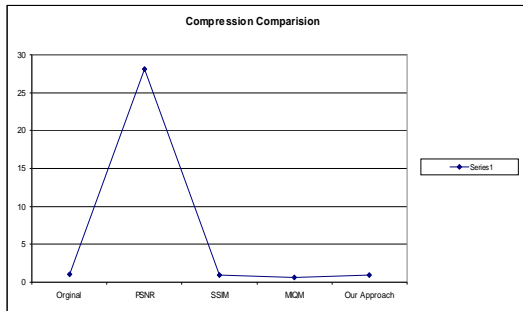


Figure 3.18: JPEG Compression Comparison with other methods

On observing the graph we can come to a conclusion that our approach values are very nearer to the value 1. So it over perform MIQM for the given images in JPEG Compression performance.

### 3.2.4 Photometric Blur Distortions

For this demonstration we consider two images as shown below



Fig. 3.19: Test images for Blur distortion

When we apply the Gaussian blur distortions with factor 12 for image (a) then it produces the distorted image and when we measure factor then it yields the measurement index as 11.16. This show our method yields accuracy of 0.93 for the image (a). When we apply the perspective distortions with factor 15 for image (b) then it produces the distorted image and when we measure factor then it yields the measurement index as 13.95 This show our method yields accuracy of 0.92567 for the image (b).

The results can be shown in below figure.



Figure 3.20: Image (a) and (b) with photometric Gaussian Blur distortions results

Table 3.5: Gaussian Blur performance measurement

Image	Applied Value	Measured Value
Girl	12	11.16
Building	A15	13.95

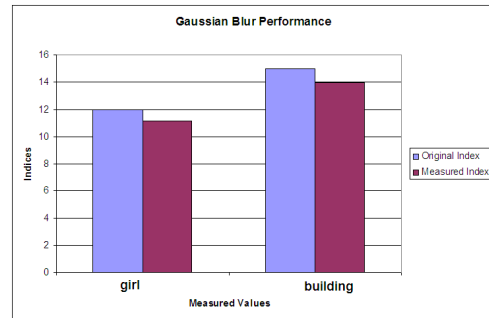


Fig. 3.21: Gaussian blur performance

On observing the graph we can come to a conclusion that our approach values are very nearer to the original image. So we can conclude that our system performance is well in Gaussian blur type of distortions.

Table 3.6: Gaussian Blur comparison with other methods

Image	Gaussian Blur				
	Original	PSNR	SSIM	MIQM	Our Approach
Girl	1	23.3433	0.7384	0.6853	0.9267

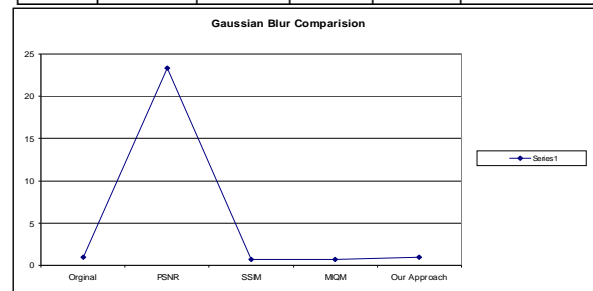


Fig. 3.22: Gaussian blur comparison

On observing the graph we can come to a conclusion that our approach values are very nearer to the value 1. So it over perform MIQM for the given image for Gaussian Blur comparison.

### REFERENCES

- [1] G. AlRegib and M. Solh "MIQM- Multi camera Image Quality Measure "IEEE transactions on image processing Vol. 21 No. 9, Sep 2012
- [2] G. AlRegib and M. Solh, "Characterization of image Distortions in multi camera system," in Proc. 2nd International Conference Immersive Telecommunication, May 2009, pp.1-7.
- [3] C. Hewage, S. Dogan, S. Worrall and A. Kondoz, "Prediction of stereoscopic video quality using objective Quality models of 2-Dimensional video," Electron. Lett. vol. 44, no. 16, pp. 963-966, Jul. 2008.
- [4] A. Tikanmaki, A. Smolic, K. Miller, and A. Gotchev "Quality assessment of 3 Dimensional video in rate allocation experiment," in Proc. IEEE Symp. Consumer Electron. Apr. 2008, pp. 2-5.

- [5] J. Starck, J. Kilner and A. Hilton “Objective quality assessment in free viewpoint video production,” in Proc. 3DTV, 2008, pp. 224–229.
- [6] L. Cui and A. Allen, “An image quality metric based on the corner, edge and symmetry maps,” in Proc. British Mach. Vis. Conference 2008, pp. 2–11.
- [7] P. Campisi, P. Callet, R. Cousseau and A. Benoit, “Quality assessment of the stereoscopic images,” in Proc. EUSIPCO, Sep. 2007, pp. 2109–2115.
- [8] N. Ozbek, E. Tunali and A. Tekalp “Rate allocation between views in scalable stereo video coding using an objective stereo video quality measure,” in Proc. ICASP, Apr. 2007, pp. 1044–1049.
- [9] A. Kubota, M. Tanimoto, C. Zhang A. Smolic, M. Magnor, and T.Chen “Multiview imaging and 3DTV,” IEEE Signal Process Magazine, volume 24, no. 6, pp. 9–22, Nov. 2007.
- [10] C. Tang, C. Tsai, and C.Yu, “Visual sensitivity guided bit allocation for video coding,” IEEE Transaction. Multimedia, volQ. 8, no. 1, pp. 11–18, Feb.2006
- [11] S. Leorin, R. Cutler and L. Lucchese, “Quality assessment of panorama video for video conferencing applications” in Proc. IEEE Workshop Multimedia Signal Process., Nov.2005, pp. 2–5.
- [12] Z. Wang, H. Sheikh, E. Simoncelli and A. Bovik, “Image quality assessment: From error visibility to the structural similarity,” IEEE Trans. Image Process., vol. 13, no. 4, pp. 599–613, Apr. 2004.
- [13] Application and Requirement for 3DAV, ISO Standard N 5877, Jul.2003.
- [14] E. H. Adelson and P. J. Burt, “A multi resolution spline with application to image mosaics,” ACM Transaction. Graph. vol. 2, no. 4, pp. 216–237, Oct.1983.
- [15] H.Baker, C.Papadas and D.Tanguay, “MultiViewpoint un-compressed capture and mosaicking with high bandwidth PC camera array,” in Proc. sixth Workshop Omnidirect. Vis., Camera Netw. Non Classical Cameras, 2005, pp. 1–9.
- [16] H.-J. Zepernick and U. Engelke and, “Perceptual based quality metrics for image and video service: A survey,” in Proc. EuroNGI, May 2007, pp. 189–198.
- [17] E. Simoncelli and Z. Wang “Translational insensitive image similarity in the complex wavelet domain,” in Proc. ICASSP, Mar. 2005, pp. 571–577.
- [18] A. Zisserman and H. Richard, Multiple View Geometry in Computer Vision. Cambridge, U.K: Cambridge Univ.Press, 2000.
- [19] H. Sheikh, Z. Wang, A. C. Bovik and L. Cormack, and. (2010). LIVE Image Quality Assessment Database Release2 [Online]. Available: <http://live.ece.utexas.edu/research/quality>
- [20] F. J. Canny, “A computational approach to edge detection,”IEEE Transaction Pattern Anal. Mach. Intell., vol. 8, no. 6, pp. 677–699, Jun. 1986.